DESIGN AND BUILD THE SLIDING DRUM COLLECTOR WITH RPM COUNTER ARDUINO FOR NANOFIBER FABRICATION

RANCANG BANGUN KOLEKTOR DRUM GESER DENGAN PENGHITUNG RPM ARDUINO UNTUK FABRIKASI NANOSERAT

Panji Setyo Nugroho, Dewa Pascal Ariyanto, Della Astri Widayani, Luluk Arifatul Hikamiah, Jasmine Cupid Amaratirta, Dewanto Harjunowibowo, Yulianto Agung Rezeki*

[1]Department of Physics Education, Faculty of Teacher Training and Education, Universitas Sebelas Maret, Surakarta, Indonesia

Email: yarezeki@staff.uns.ac.id

ABSTRACT

The rotational speed of the drum collector is an important parameter to determine the morphology of the nanofiber. Currently, many researchers are modifying single nozzle into multi-nozzle to obtain a wide range of materials. However, it requires more powerful syringe-pumps or increasing their number, leading to escalated cost. In addressing this issue, the sliding drum collector with an RPM counter is proposed as a solution. This apparatus uses a DC motor 775 and a stepper motor Nema17 as the driving device and an IR-sensor as the RPM counter. The RPM counter on this apparatus has also been calibrated and obtained an accuracy value of 97.87% and a precision value of 96.45%. The performance of the sliding drum collector has been validated. The sliding drum collectors have been proven to produce wider material with an area of (389 ± 8) cm^2, (66 ± 18) cm^2 larger than an ordinary drum collector.

Keywords: drum collector, RPM counter Arduino, rotational speed, accuracy, precision

ABSTRAK

Kecepatan rotasi kolektor drum merupakan parameter penting untuk menentukan morfologi nanoserat. Saat ini, banyak peneliti yang memodifikasi nosel tunggal menjadi nosel ganda untuk mendapatkan berbagai macam bahan. Namun demikian, hal ini memerlukan pompa jarum suntik yang lebih kuat atau meningkatkan jumlahnya yang menyebabkan peningkatan biaya. Untuk mengatasi masalah ini, kolektor drum geser dengan penghitung RPM diusulkan sebagai solusi. Alat ini menggunakan motor DC 775 dan motor stepper Nema17 sebagai perangkat penggerak dan sensor IR sebagai penghitung RPM. Penghitung RPM pada alat ini juga telah dikalibrasi dan memperoleh nilai akurasi sebesar 97,87% dan nilai presisi sebesar 96,45%. Kinerja kolektor drum geser telah selesai divalidasi. Kolektor drum geser telah terbukti menghasilkan material yang lebih luas dengan luas area (389 ± 5) cm^2, (66 ± 13) cm^2 lebih besar dari kolektor drum biasa.

Kata Kunci: *kolektor drum, penghitung RPM Arduino, kecepatan putar, akurasi, presisi*

1. INTRODUCTION

Nanofibers has many advantages over conventional materials. Nanofibers has a large surface area and has high mechanical properties (Sanchaniya et al., 2022). Nanofibers that are currently developed are made from polymer and additives to obtain certain properties. For example, polyvinyl alcohol and soursop leaf extract have been shown to have good potential antibacterial activity (Aruan et al., 2017). Then, PVA and hydroxipatile are utilized for bone tissue engineering (Hartatiek et al., 2020). Nanofiber fabrication in the electrospinning process is influenced by several parameters. These parameters are divided into three types, namely process parameters, solution parameters, and environmental parameters. These three parameters greatly affect the morphology and size of the particles formed (Rezeki, 2020). Process parameters in electrospinning are voltage (Rosman et al., 2020; Shin et al., 2018), distance tip to collector (Ibrahim & Klingner, 2020), flow rate (Al-Okaidy & Waisi, 2023; Sandri et al., 2020), and revolution speed of collector (Al-Okaidy & Waisi, 2023; Sanchaniya et al., 2022). Solution parameters in electrospinning are density, viscosity, conductivity, and surface tension (Rezeki, 2020). The last parameter is environmental parameters affected the solvent evaporation, divided into temperature and humidity (Tan et al., 2022).

The rotation speed of the collector affects the diameter size of the nanofiber. Increasing the collector rotation speed will reduce the nanofiber diameter size (Yao et al., 2014; Yousefzadeh, 2017). As the rotation speed increases, the solvent evaporation rate will increase, resulting in nanofibers with smaller diameter and higher crystallinity formed on the drum collector (Yousefzadeh, 2017). This statement is proven by an experiment conducted by Al-Okaidy & Waisi (2023), who increased the collector rotation speed from 70 rpm to 210 rpm that produced a fiber size that decreased from 260 nm to 175 nm.

For now, electrospinning has had many modifications from its inception. One of them is multi-nozzle electrospinning (Nuryantini et al., 2014). The results of the experiments showed differences in the thickness of the resulting nanofibers. In studies using multi-nozzle, a powerful syringe pump or even more syringe pumps are required to pump the solution. This will delay the production rate of nanofiber and more costly. To overcome this limitation, this study proposed to develop the sliding drum collector with

an RPM counter using Arduino. The proposed tool aims to fabricate nanomaterials that are more stable and have a wider surface area.

2. METHODS

2.1 Research Design

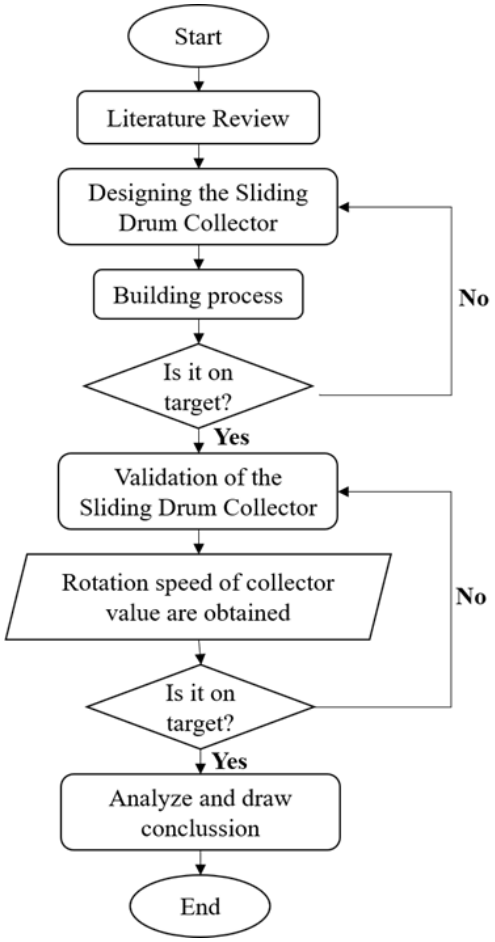

Figure 1. Research methodology

Research on sliding drum collectors (SDC) is a development of previous research with research stages, as shown in Figure 1. Literature studies was obtained from journals and component datasheets. The sliding drum collector was designed with an RPM counter using Arduino, taking into account the latest innovations based on previous research. The designed system considers aspects of mechanical components and electrical components. The system that was built was collected, processed, calibrated, validated, performance test, and analyzed the data until the conclusion was obtained.

The work of the sliding drum collector with an RPM counter using Arduino flowed in Figure 2.

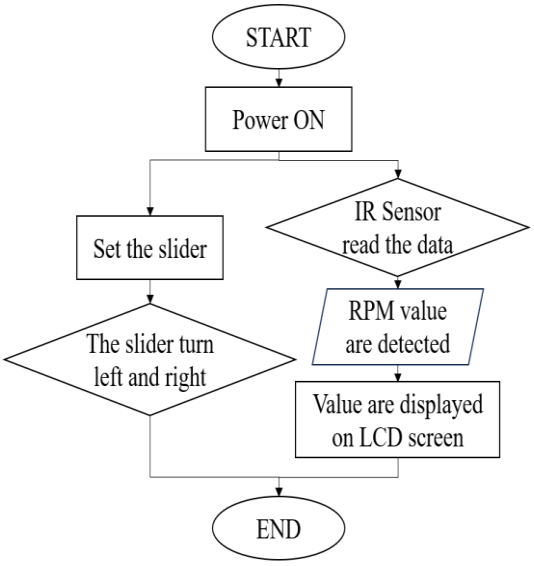

Figure 2. Research design

The rotational speed of drum collector is adjusted using Pulse Width Monitor (PWM). Then, the value of collector speed was measured using the infrared sensor. The value detected had to pass calibration and validation to obtain the best measurement results and determine the feasibility of the measuring instrument. Then, the detection result was displayed on the LCD screen.

The sliding drum collector used a Nema17 Stepper motor to move right and left. The speed of sliding could be input by pushing the keypad button. The sliding drum collector had to pass validation to obtain the best performance.

2.2 Design and Construction of SDC Device

The sliding drum collector used several devices from the design to the validation stage. Arduino IDE was used for software development by the system developers. Meanwhile, the hardware used for development was shown in Table 1 and Table 2

Table 1. Mechanical Tools

Num.	Materials	Qty.
1	Alumunium round bar	1
2	Alumunium plate	1
3	Bearing SC12UU	4
4	DC motor 775	1
5	Linear shaft 12mm	2
6	Nema 17 stepper motor	1
7	Pillow block	2
8	Rail shaft SK12UU	4
9	Bracket motor	2
10	Bracket belt	1
11	Iddler pulley	1
12	Pillowblock	2
13	Pulley 20 teeth	2
14	Pulley 60 teeth	1
15	Timing belt GT2 closed loop	1
16	Timing belt GT2 open loop	1

Table 2. Electrical tools

Num.	Materials	Qty.
1	Arduino UNO R3	1
2	LCD 16x2	1
3	Keypad membrane 4x4	1
4	Pulse Width Modulation (PWM)	1
5	Micro controller box	1
6	Infrared sensor	1

Then, the sliding drum collector was built following the design shown in Figure 3 and Figure 4. The electrical circuit of SDC was made following the design shown in Figure 5.

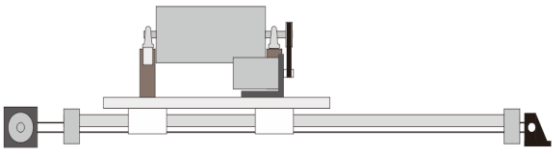

Figure 3. Mechanical Design Front View

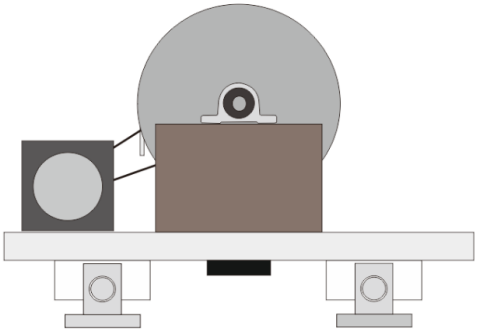

Figure 4. Mechanical Design Side View

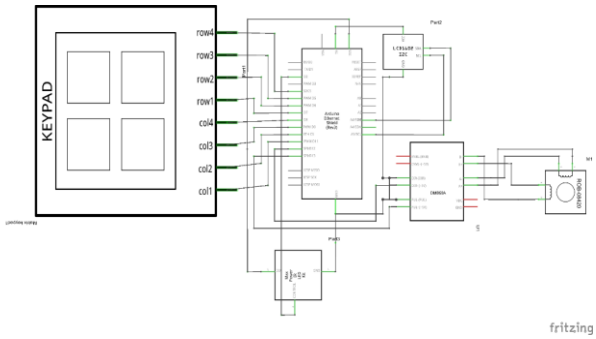

Figure 5. Circuit Design

2.3 Data Validation Technique

The RPM Counter had been built along with the SDC before. Then, the RPM Counter was tested and calibrated to obtain valid data. The RPM Counter Arduino obtained the revolutions per minute (rpm) value from the Arduino count. The data's value was validated against the AR926 Smart Sensor Digital Tachometer measurement standard. Validation was considered complete after going through error, accuracy, and precision analysis. Then, the performance of the SDC will be validated using a performance test.

Accuration analysis

Measurement is inherently intertwined with error, a concept acknowledged in scientific discourse. Accuracy is the closeness of measurement results and actual values (Perea Martins, 2019). Before calculating accuracy, it is required to calculate the error first. Error is the difference between the measured value and the reference value, shown by equation:

$$\text{Error} = Y_n - X_n \quad \text{.....} \quad [1]$$

The level of accuracy indicates how reliable the measurement methods are. To calculate the accuracy level, the equation used is as follows:

$$\text{Accuracy} = \left(1 - \frac{\text{Error}}{Y_n}\right) \times 100\% \ \text{...} \quad [2]$$

where,

X_n is calculated value (rpm),

Y_n is actual value (rpm) from measurement calibrator (Putra et al., 2022).

Precision analysis

Precision is the match between the value of the measured quantity obtained by repeated measurements on the same object (Perea Martins, 2019). The value of precision can be calculated by knowing the standard deviation and relative standard deviation first. From Gao et al. (2013) we know that:

$$\bar{x} = \frac{\sum_{i=1}^{n} x_i}{n} \quad \text{.....} \quad [3]$$

$$SD = \sqrt{\frac{1}{n-1} \sum_{i=1}^{n} (x_i - \bar{x})^2} \quad \text{.....} \quad [4]$$

From Gao et al. (2013) equation of Relative Standar Deviation (RSD) and precision can be written as:

$$RSD = \frac{SD}{\bar{x}} \times 100\% \quad \text{.....} \quad [5]$$

$$\text{Precision} = 100\% - RSD \quad \text{.....} \quad [6]$$

where,

SD is standar deviation (rpm)

$\bar{x}$ is mean of the data.

Peformance Test

The performance validation of the SDC was done by conducting three experiments with different collector treatments. The first experiment was a stationary collector, the second experiment used a rotating drum collector, and the last used a rotating and sliding drum collector. These experiments used the same control variables, which are: solution (PVA with a concentration of 10wt.%), running time (1 hour), voltage (23 kV), and distance tip to collector (15 cm). The nanofiber area formed on the collector was calculated using equation [7] and equation [8]. Diameter, length, and width were each five times measured. The SD was calculated using equation [4]. Then, the uncertainty was calculated using equation [9]. After that, the results of three experiments will be compared so it will be seen which collector produces the largest area (*A*).

$$A_{circle} = \pi r^2 \quad \text{.....} \quad [7]$$

$$A_{rectangle} = \text{length} \times \text{width} \quad \text{.....} \quad [8]$$

$$U = \frac{SD}{\sqrt{n}} \quad \text{.....} \quad [9]$$

3. RESULTS AND DISCUSSION

3.1 SDC Build Result

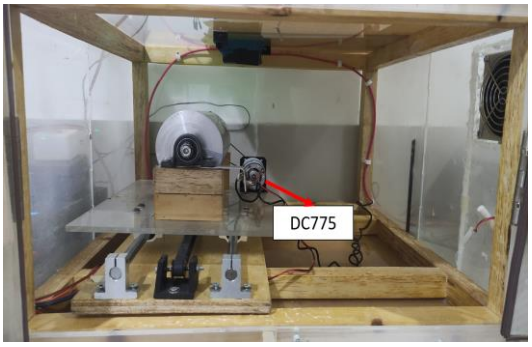

Figure 6. Result of SDC front view

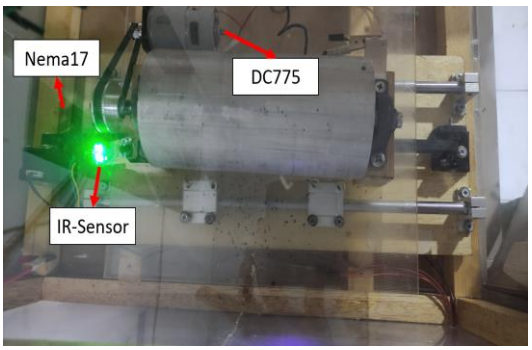

Figure 7. Result of SDC top view

The sliding drum collector with an RPM counter using arduino has been successfully built following initial design and is ready to the next stage. Figure 6 and Figure 7 show the view of the sliding drum collector from above and from the side respectively.

3.2 IR RPM Counter Calibration Performance

The infra-red sensor as the core detector for the RPM counter needs to be calibrated in order to get accurate results. The calibrator used in this experiment is the Smart Sensor AR926 Digital Tachometer. The data shown by

the RPM counter will be compared with the data obtained from the calibrator tachometer. The data before calibration is shown in the **Error! Reference source not found.**.

Table 3. Accuracy Data Before Calibration

Value of PWM (%)	AR926 (RPM)	IR Arduino (RPM)	Error (%)
12	50.18	60.00	23.24
13	88.90	96.80	13.28
14	120.12	124.80	4.07
15	149.38	156.00	6.00
16	172.02	177.60	5.45
17	200.84	206.40	2.77
18	227.20	232.80	2.66
19	253.60	256.80	2.10
20	285.44	285.60	1.57
21	305.80	319.20	4.38
22	337.60	343.20	1.85
		Mean (%)	**6.12**
		Accuracy (%)	**93.68**

Precision validation of the RPM Counter data is compared with data from AR926. The precision value is sought based on 5 times of data collection with PWM signal duty cycle range from 12% to 22%. Precision is calculated based on the value of standard deviation and relative standard deviation. The precision value of the data can be seen in the Table 4.

Table 4. Precision data before calibration

Value of PWM (%)	SD	RSD	Precision (%)
12	12.00	0.20	80.00
13	14.81	0.15	84.71
14	6.57	0.05	94.73
15	8.49	0.05	94.56
16	10.04	0.06	94.35
17	5.37	0.03	97.40
18	6.57	0.03	97.18
19	6.57	0.03	97.44
20	5.37	0.02	98.12
21	6.57	0.02	97.94
22	6.57	0.02	98.08
		RSD (%)	**5.95**
		Average Precision (%)	**94.05**

This method uses the standard deviation measurement and the average of the measurement data.

Then the data that has been obtained is processed into a graph and analyzed so that the linear regression equation is obtained. Before calibration, the following graph in Figure 8 was obtained.

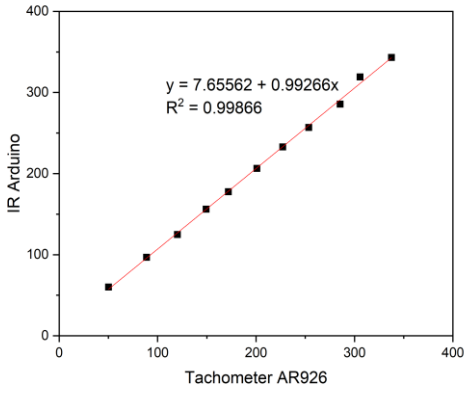

Figure 8. Regression Chart Before Calibration

Equation [10] shows the linier regression equation obtained from Figure 8.

$$y = 7.65562 + 0.99266x \quad \textbf{.....} \quad \textbf{[10]}$$

The x-axis value is the average value of a number of data obtained based on the values listed on the calibrator. Then the y-axis value is the average value of a number of data obtained from the RPM counter calculation.

Based on Chicco et al. (2021) the R-square value indicates the proportion of variance in the dependent variable that can be predicted by the independent variable (with best value +1). The closer to 1, the better the prediction results. Based on the data, the r-square value shows a value of 0.99866. This shows the percentage of the dependent variable explained by the independent variables in this model.

Based on Bangdiwala (2018), the linear regression can determine the relationship between the independent variable X and the dependent variable Y. The slope value can measure the relationship between X and Y. If the value is 0, then there is no relationship between these variables. If the value is negative, then the values of the X and Y variables are reversely proportional. If the value is positive, then the values of variables X and Y will be directly proportional. The concept is used in the calibration process in this tool where the independent variable (X-axis) is the calibrator and the dependent variable (Y-axis) is the measured value. By keeping the slope value close to 1, the measured value will be close to the value of the calibrator.

Then the slope value was obtained as 0.99266. This shows that the value of the dependent variable is almost the same as the independent variable. Last, an intercept value was obtained as 7.65562. This shows that the difference in the value of the independent and dependent variables at point (0.0) is 7.65562. After obtaining the regression equation, the existing coding on the Arduino is re-adjusted.

3.3 Post Calibration IR RPM Counter Performance

After calibrating, data is obtained with 20 repetitions of data collection for each value in PWM. The average value of the data can be seen in the Table 5.

Table 5. Data after calibration

Value of PWM (%)	AR926 (RPM)	IR Arduino (RPM)	Error (%)
12	54.40	55.74	5.32
13	92.62	90.43	4.13
14	121.04	119.00	2.74
15	149.80	148.41	2.47
16	188.74	188.86	2.19
17	213.80	212.65	2.00
18	242.11	243.00	1.25
19	278.88	279.00	0.60
20	306.04	306.00	1.02
21	340.23	341.40	1.29
22	350.21	350.40	0.40
		Mean (%)	**2.13**
		Accuracy (%)	**97.87**

Based on the calculation obtained mean of standard error is 2.13% and measurement accuracy of 97.87%. Increase from the previous accuracy of 93.88%. This indicates the more accurate the measurement results of the RPM counter.

The precision validation of RPM Counter data is compared with data from AR926. The precision value is sought based on 20 times of data collection with a signal range of 12-22%. Precision is calculated based on the value of standard deviation and relative standard deviation. The precision value of the data can be seen in the Table 6.

Table 6. Precision data after calibration

Value of PWM (%)	SD	RSD	Precision (%)
12	5.68	0.10	89.80
13	4.47	0.05	95.06
14	6.16	0.05	94.83
15	4.76	0.03	96.79
16	5.74	0.03	96.96
17	5.42	0.02	97.45
18	6.60	0.27	97.28
19	5.33	0.02	98.09
20	3.89	0.01	98.73
21	8.24	0.02	97.59
22	5.64	0.02	98.39
		RSD (%)	**3.55**
		Average Precision (%)	**96.45**

Based on the calculation, the precision value in data collection is 96.45%. Increase from previous precision of 94.05%. This indicates the measurement results of the RPM counter arduino are more precise.

Then the data that has been obtained is processed into a graph and analyzed so that the linear regression equation is obtained. After calibration, the following graph in Figure 9 is obtained.

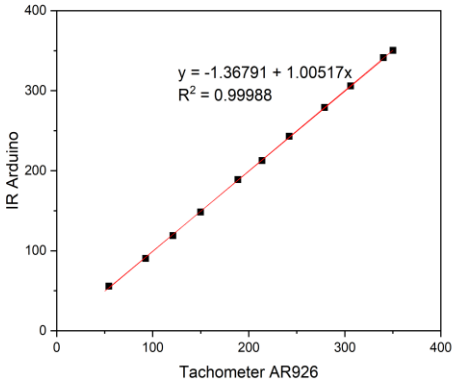

Figure 9. Regression chart after calibration

Equation [11] shows the linier regression equation obtained from Figure 9.

$$y = -1.36791 + 1.00517x \quad \text{.....} \quad [11]$$

The slope value on the graph is 1.00517. A slope value close to 1 indicates that the calibrated instrument gives accurate results. The slope value before calibration is 0.99266 and after calibration the value is close to 1 with a value of 1.00517. So the arduino RPM counter has been calibrated. Then the intercept value is obtained -1.36791 down from the previous intercept which is 7.65562. This indicates that after calibration, the difference in the value of the independent variable and the dependent variable at point (0,0) is decreasing towards zero. This indicates that the offset value between the independent variable and the dependent variable is decreases.

3.4 Result of SDC Performance

The performance of the drum collector was tested using PVA 10% solutions with applied voltage is 23 kV and the distance from the needle to the collector is 15 cm for three types of drum collector. The first experiment was a stationary collector, the second experiment used a rotating drum collector, and the last used a rotating and sliding drum collector. Data collection was carried out five times in each experiment.

First Experiment Result

The area of nanofibers formed is marked with a red circle in Figure 10. Based on the experiment, the formation of nanofiber is centered in the middle. This is shown by the edges of the nanofiber which are thinner than the center. Due to the shape of the nanofiber formed is a circle, the area formed is calculated using equation [7]. The results of area measurement can be seen in Table 7.

Figure 10. First experiment result

Table 7. Measurement of First Experiment

Number of Measurement	Diameters (cm)
1	12.0
2	12.0
3	11.4
4	11.7
5	10.2
Average (cm)	**11.4**
SD (cm)	**0.7**
Uncertainty (cm)	**0.3**

Second Experiment Result

This result produces a larger nanofiber area than the previous experiment shown in Figure 11. However, the formation of nanofiber is still centered in the middle. Due to the shape of the nanofiber formed is a rectangle, the area formed is calculated using equation [8]. The results of area measurement can be seen in Table 8.

Figure 11. Second experiment result

Table 8. Measurement of Second Experiment

Number of Measurement	Length (cm)	Width (cm)
1	28.4	12.0
2	28.0	10.7
3	28.8	11.5
4	28.4	11.1
5	28.4	11.5
Average (cm)	**28.4**	**11.4**
SD (cm)	**0.3**	**0.5**
Uncertainty (cm)	**0.1**	**0.2**

Third Experiment Result

This result produces the largest nanofiber area of the previous experiments shown in Figure 12. The thickness of the nanofiber is also equally distributed, compared to the previous experiments. Same as the previous experiment, the area of the nanofiber formed was calculated using equation [8]. The result of area measurement can be seen in Table 9.

Figure 12. Third experiment result

Table 9. Measurement of Third Experiment

Number of Measurement	Length (cm)	Width (cm)
1	28.0	13.5
2	28.5	14.0
3	28.0	14.0
4	28.0	13.5
5	28.3	14.0
Average (cm)	**28.2**	**13.8**
SD (cm)	**0.2**	**0.3**
Uncertainty (cm)	**0.1**	**0.1**

The three experiments were conducted with different methods and resulted in different material areas. The comparison of material area in each experiment can be seen in Table 10.

Based on the experimental results, the first experiment has an area (286 ± 11) cm^2 smaller than third experiment. In the second and third experiments there is a difference in area calculation of about (66 ± 13) cm^2. Then, the visible eye can see that second experiment has a different thickness between the center and the sides. Whereas in third experiment, it looks equally thick and wider. Based on this, it can be concluded that third experiment produces the most extensive material with an equal thickness.

Table 10. Comparison The Result of Collector

Experiment	Dimension			
	Diameter (cm)	Length (cm)	Width (cm)	Area (cm^2)
1	11.5 ± 0.3	-	-	103 ± 6
2	-	28.4 ± 0.1	11.4 ± 0.2	323 ± 8
3	-	28.2 ± 0.1	13.8 ± 0.1	389 ± 5

4. CONCLUSION

RPM counter has been calibrated using AR926 digital tachometer. After calibration, the accuracy value increased from 93.88% to 97.87%. Then the precision value increases from 94.05% to 96.45%. Based on the simple linear regression graph, after calibration the intercept value drops from 7.65562 to -1.36791. Then the slope value is getting closer to 1 with the value before calibration is 0.99266 after calibration to 1.00517. This shows that the performance after calibration is better. The performance of the sliding drum collector has been validated. The sliding drum collectors have been proven to produce wider material with an area of (389 ± 5) cm^2, (66 ± 13) cm^2 larger than an ordinary drum collector.

5. ACKNOWLEDGEMENTS

The authors thank the Universitas Sebelas Maret through the Research Group Research Grant (Grant No. 228/UN27.22/PT.01.03/2023) for financial support.

6. REFERENCES

Al-Okaidy, H. S., & Waisi, B. I. (2023). The Effect of Electrospinning Parameters on Morphological and Mechanical Properties of PAN-based Nanofibers Membrane. *Baghdad Science Journal*. https://doi.org/10.21123/bsj.2023.7309

Aruan, N. M., Sriyanti, I., Edikresnha, D., Suciati, T., Munir, M. M., & Khairurrijal, K. (2017). Polyvinyl Alcohol/Soursop Leaves Extract Composite Nanofibers Synthesized Using Electrospinning Technique and their Potential as Antibacterial Wound Dressing. *Procedia Engineering*, *170*, 31–35. https://doi.org/10.1016/j.proeng.2017.03.006

Bangdiwala, S. I. (2018). Regression: simple linear. *International Journal of Injury Control and Safety Promotion*, *25*(1), 113–115. https://doi.org/10.1080/17457300.2018.1426702

Chicco, D., Warrens, M. J., & Jurman, G. (2021). The coefficient of determination R-squared is more informative than SMAPE, MAE, MAPE, MSE and RMSE in regression analysis evaluation. *PeerJ Computer Science*, *7*, 1–24. https://doi.org/10.7717/PEERJ-CS.623

Gao, Y., Ierapetritou, M. G., & Muzzio, F. J. (2013). Determination of the confidence interval of the relative standard deviation using convolution. *Journal of Pharmaceutical Innovation*, *8*(2), 72–82. https://doi.org/10.1007/s12247-012-9144-8

Hartatiek, Yudyanto, Wuriantika, M. I., Utomo, J., Nurhuda, M., Masruroh, & Santjojo, D. J. D. H. (2020). Nanostructure, porosity and tensile strength of PVA/Hydroxyapatite composite nanofiber for bone tissue engineering. *Materials Today: Proceedings*, *44*, 3203–3206. https://doi.org/10.1016/j.matpr.2020.11.438

Ibrahim, H. M., & Klingner, A. (2020). A review on electrospun polymeric nanofibers : Production parameters and potential applications. *Polymer Testing*, *90*(May), 106647. https://doi.org/10.1016/j.polymerte

sting.2020.106647

Liyanage, A. A. H., Biswas, P. K., Dalir, H., & Agarwal, M. (2023). Engineering uniformity in mass production of MWCNTs/epoxy nanofibers using a lateral belt-driven multi-nozzle electrospinning technique to enhance the mechanical properties of CFRPs. *Polymer Testing*, *118*(September 2022), 107883. https://doi.org/10.1016/j.polymertesting.2022.107883

Nuryantini, A. Y., Munir, M. M., Ekaputra, M. P., Suciati, T., & Khairurrijal. (2014). Electrospinning of poly(vinyl alcohol)/chitosan via multi-nozzle spinneret and drum collector. *Advanced Materials Research*, *896*, 41–44. https://doi.org/10.4028/www.scientific.net/AMR.896.41

Perea Martins, J. E. M. (2019). Introducing the concepts of measurement accuracy and precision in the classroom. *Physics Education*, *54*(5). https://doi.org/10.1088/1361-6552/ab3143

Putra, M. E., Gizi, J., Masyarakat, F. K., Andalas, U., Studi, P., Mesin, T., & Andalas, U. D. (2022). Akurasi Dan Presisi Alat Ukur Tinggi Badan Digital Untuk Penilaian Status Gizi. *Jurnal Endurance*, *6*(3), 616–621. https://doi.org/10.22216/jen.v6i3.580

Rezeki, Y. A. (2020). *Pabrikasi Partikel Nano Ekstrak Kulit Manggis sebagai Antioksidan Menggunakan Teknik Electrospray*. Institut Teknologi Bandung.

Rosman, N., Wan Salleh, W. N., Jamalludin, M. R., Adam, M. R., Ismail, N. H., Jaafar, J., Harun, Z., & Ismail, A. F. (2020). Electrospinning parameters evaluation of PVDF-ZnO/Ag2CO3/Ag2O composite nanofiber affect on porosity by using response surface methodology. *Materials Today: Proceedings*, *46*(xxxx), 1824–1830. https://doi.org/10.1016/j.matpr.2020.11.847

Sanchaniya, J. V., Kanukuntla, S. P., Simon, S., & Gerina-Ancane, A. (2022). Analysis of Mechanical Properties of Composite Nanofibers Constructed on Rotating Drum and Collector Plate. *Engineering for Rural Development*, *21*, 737–744. https://doi.org/10.22616/ERDev.2022.21.TF227

Sandri, G., Rossi, S., Bonferoni, M. C., Caramella, C., & Ferrari, F. (2020). Electrospinning Technologies in Wound Dressing Applications. *Therapeutic Dressings and Wound Healing Applications*, 315–336. https://doi.org/10.1002/9781119433316.ch14

Shin, D., Kim, J., & Chang, J. (2018). Experimental study on jet impact speed in near-field electrospinning for precise patterning of nanofiber. *Journal of Manufacturing Processes*, *36*(June), 231–237. https://doi.org/10.1016/j.jmapro.2018.10.011

Tan, S. M., Teoh, X. Y., Le Hwang, J., Khong, Z. P., Sejare, R., Almashhadani, A. Q., Assi, R. A., & Chan, S. Y. (2022). Electrospinning and its potential in fabricating pharmaceutical dosage form. *Journal of Drug Delivery Science and Technology*, *76*(August), 103761. https://doi.org/10.1016/j.jddst.2022.103761

Yao, J., Bastiaansen, C. W. M., & Peijs, T. (2014). High strength and high modulus electrospun nanofibers. *Fibers*, *2*(2), 158–187. https://doi.org/10.3390/fib2020158

Yousefzadeh, M. (2017). Modeling and simulation of the electrospinning process. In *Electrospun Nanofibers*. Elsevier Ltd. https://doi.org/10.1016/B978-0-08-100907-9.00012-X